# Supporting Information

Bioactive tissue derived nanocomposite hydrogel for permanent arterial embolization and enhanced vascular healing

*Jingjie Hu, Izzet Altun, Zefu Zhang, Hassan Albadawi, Marcela A. Salomao, Joseph L. Mayer, L.P. Madhubhani P. Hemachandra, Suliman Rehman, and Rahmi Oklu**

**Experimental Section**

*Decellularization of Porcine Heart:* Fresh porcine hearts were obtained from deceased pigs approved by Institutional Animal Care and Use Committee, Mayo Clinic, for decellularization. The left ventricle was collected and decellularized following an established protocol.[36] Briefly, the cardiac tissue was first rinsed with DI water for 45 minutes, followed by 1 % (wt/vol) sodium dodecyl sulfate (SDS) (Fisher Scientific, Cat. # BP166) (in phosphate-buffered saline (PBS)) wash for 4-5 days. SDS detergent was changed every 24 hours until the tissue was fully decellularized and turned completely white. Finally, decellularized cardiac tissue was washed in DI water for two days (with constant water change) to ensure the complete removal of SDS. A sample of cardiac tissue at day 0, 3, and 5, respectively, were collected and embedded in paraffin for histological analysis. The cardiac specimen was sectioned into 4 μm slices and stained with hematoxylin and eosin (H&E) to confirm the removal of cells. Lastly, the cardiac tissues were frozen at -80 °C before being lyophilized (Labconco, 0.120 mBar, and -50 °C) and stored at 4 °C.

*Preparation of ECM:* Lyophilized cardiac tissue was solubilized in 1 mg $mL^{-1}$ pepsin (Sigma Aldrich, Cat. # 9001-75-6) (in 0.1M HCl), and underwent continuous digestion with vigorous agitation for 2 days to achieve a homogenous solution (25 mg $mL^{-1}$). The solution was then brought to pH 7.6 by adding 1M sodium hydroxide (NaOH), forming ECM solution. The final ECM solution (~20 mg $mL^{-1}$) was used freshly for characterization and ECM gel formation.

*ECM Protein Extraction:* Protein in final ECM solution (after digestion and neutralization) was extracted into protein extraction buffer containing protease and phosphatase inhibitors. The samples were centrifuged at 12000 RPM at 4 °C for 10 minutes. The supernatant was transferred to a new tube for protein quantification using a Bicinchoninic Acid (BCA) Protein Quantification protein kit (Thermo Scientific, Prod. # 23225), according to the manufacturer's instructions. Briefly, extracted protein (25 µL) was mixed with 200 µL BCA working reagent and incubated at 37 °C for 30 minutes. Absorbance was measured at 562 nm using a microplate reader (SpectraMax iD5, Molecular Devices).

*Double-stranded DNA (dsDNA) Quantification*: The amount of dsDNA in the native left ventricular tissue and in the ECM solution after decellularization was evaluated. Briefly, dsDNA was extracted using a standard DNA isolation kit (NuceloSpin, Macherey-Nagel, Düren, Germany) according to manufacturer's instruction. The amount of extracted dsDNA was measured using a Nanodrop spectrophotometer (Thermo Fisher Scientific, Waltham, MA) at 260 nm wavelength. The tests were run in triplicate.

*Sodium Dodecyl Sulfate–Polyacrylamide Gel Electrophoresis (SDS-PAGE)*: Proteins extracted from ECM were loaded into 8-16 % sodium dodecyl sulfate-polyacrylamide gel (Bio-Rad, Cat. # 456-8104) and separated by electrophoresis. 15 µg of total ECM protein was loaded into each

well of the polyacrylamide gel and compared to rat tail collagen type I (Corning, Cat. # 354236). The polyacrylamide gel was then stained with Imperial™ Protein Stain for visualization (Thermo Scientific, Prod. # 354236).

*Turbidimetric Gelation Kinetics:* Turbidimetric gelation kinetics of ECM were performed and analyzed according to a previously established protocol.[36] 100 µL of 9, 12, and 20 mg $mL^{-1}$ cold ECM solution (n=4) was loaded into a 96 well-plate in a microplate reader that was pre-heated to 37 °C. The reading was recorded every 30 seconds for 90 minutes. The normalized absorbance (NA) was calculated according to Equation S1, where $A$ is the absorbance at a given time, $A_0$ is the absorbance at point 0, and $A_{max}$ represents the maximum absorbance.

$$NA = \frac{A - A_0}{A_{max} - A_0} \qquad Equation\ S1$$

For kinetic analysis, the time needed to reach 50 % $A_{max}$ is defined as $t_{1/2}$; the lag phase, $t_{lag}$, was determined as the x-intercept by extrapolating the linear portion of the turbidimetric curve; and the slope of the curve was calculated as the speed of gelation, $S$.

*Dynamic light scattering*: The hydrodynamic size of nanoclay (NC) was obtained using dynamic light scattering (DLS) (Wyatt Mobius). DLS was carried out with the NC dispersed in ultrapure water. Prior to DLS measurement, NCs were vortexed, sonicated, and then equilibrated for 5 min. DLS distribution is the average result of 3 independent samples with 9 repetitive measurements of each sample.

*Preparation of the Nanocomposite Hydrogels:* ECM-NC gels were made by mixing neutralized ECM solution (20 mg $mL^{-1}$), 9 % (w/v) NC (Laponite XLG, BYK USA Inc., Rochester Hills, MI) and molecular biology grade water (Phenix Research Products, Candler, NC) at different

weight ratios, shown in table S1 and S2. Omnipaque (350 mgI $mL^{-1}$, GE Healthcare) was introduced into ECM-NC gels at 27 % w/w of iohexol for radiopacity, shown in table S3. The homogenous mixing of ECM-NC gels was achieved by using a SpeedMixer (FlackTek Inc., Landrum, SC).

*Rheology*: All rheological measurements were performed with a strain-controlled MCR 302 rheometer (Anton Paar USA Inc., Torrance, CA). A 25 mm diameter sandblasted aluminum upper disk and an aluminum lower plate were used, and the gap in between was kept at 1 mm for all measurements. In addition, a solvent trap was used, and the edge of the solvent trap was filled with water to provide a humidified environment to prevent drying.

For ECM solutions, large-amplitude oscillation sweep (LAOS) were performed at 10 rad $s^{-1}$. The gelation kinetics was examined using an isothermal test at a fixed strain of 0.5 % at 37 °C. The shear rate sweeps of 20 mg $mL^{-1}$ ECM solution were carried out at both 4 °C and 37 °C to assess its shear-thinning properties before and after gelation.

For ECM-NC gels, all rheological tests were performed at 37 °C unless otherwise denoted, following established protocols.[8] Shear rate sweeps performed to characterize the gel's shear thinning behavior. LAOS were performed at both 25 °C and 37 °C at a fixed angular frequency of 10 rad/s. The above tests were run in triplicates. The yield stress was calculated from LAOS. Specifically, critical strain ($\varepsilon_c$) defined as the intersection of the segmented linear fittings on the stress-strain curve, was first measured. Yield stress, $\sigma_y$, was then extrapolated as the stress value corresponding to $\varepsilon_c$. During frequency sweeps, a strain range of 0.1 to 100 rad $s^{-1}$ was scanned at a fixed strain of 0.5 % (in the linear viscoelastic region). Lastly, thixotropic test was conducted at 37 °C at 10 rad $s^{-1}$ to evaluate time-dependent shear thinning property. The strain was oscillated

between 100 % (for 1 minute) and 0.5 % (for 2 minutes) to examine the recoverability of the gels.

*Injectability***:** The injectability of ECM-NC gels through clinical catheters was investigated according to a previously developed protocol using a mechanical tester (Instron, Norwood, MA).[8] The force required for ECM-NC gels (loaded into a 1cc BD syringe) to pass a 2.8 F, 110 cm catheter (Terumo Medical Corporation, Somerset, NJ) at a flow rate of 1 mL $min^{-1}$ was recorded using Bluehill version 3 Software (Instron, Norwood, MA, US). Afterward, both break loose force and injection force were analyzed.

*Cell Culture*: L-929 mouse fibroblasts (ATCC, Manassas, VA) were cultured at 37 °C in 5 % $CO_2$ atmosphere in the following medium: Eagle's Minimum Essential Medium (ATCC, Cat. # 30-2003), 10 % Fetal Bovine Serum, and 1% Penicillin-Streptomycin.

*Cell Culture on xECM 4.5 NC Coated Plates*: To assess cell viability in direct contact with *xECM 4.5 NC*, the gels were first spread on the bottom of 96-well plate by centrifugation at 1500 RPM for 3 minutes for complete coverage. L929 cells were seeded in at a density of 5000 each well directly on top of the gel and incubated at 37 °C overnight. The cell viability was accessed using CellTiter-Glo Luminescent assay (Promega, Cat. # G7572) according to the manufacturer's instructions. After the cells were lysed, the top aliquot was carefully transferred into an opaque bottom plate, and the luminescent signal was read on a microplate reader immediately. The wells coated with gels but without cells were used as corresponding controls to each material to subtract the luminescent background from the readings. Three independent experiments were conducted with six replicates in each experiment.

*In Vitro Cytotoxicity*: *In vitro* cytotoxicity evaluation of ECM, NC, EMH, and EMH-I were conducted according to ISO-10993-5.[37] Briefly, 1g of each material were dissolved in complete cell culture medium and incubated at 37 °C for 24 hours. The supernatant and its series dilution (100 %, 50 %, 25 %, and 12.5 %) were prepared as treatment medium. In a 96-well plate, L-929 cells were seeded at a density of 5000 cells per well. After 24 hour incubation, the culture medium was aspirated and replaced with treatment medium (100 µL per well) for another 24 hours. Cell viability was analyzed using WST-1 reagents (Cayman Chemical, Ann Arbor, MI) according to the manufacturer's protocol. Briefly, WST-1 solution was added to each well (10 µL), and the plate was incubated at 37 °C for 2 hours, followed by reading the absorbance at 450 nm. Dimethyl sulfoxide (DMSO) (10 %) was used as a positive control for cytotoxicity. Three independent experiments were conducted with four replicates in each experiment.

*Antibacterial Activity*: The antibacterial activity of EMH and EMH-I was tested using Escherichia coli (*E. coli*) according to an established protocol with minor modifications.[38] A 10 mL *E. coli* suspension with a concentration of $10^7$ CFU $mL^{-1}$ was added on top of the 1 mL gel to reach a final concentration of $10^8$ CFU per milliliter gel. Gels with Luria-Bertani (LB) broth were used as negative controls. The groups were incubated for 24 hours at 37 °C at 180 rpm in a shaker incubator. The optical density of the suspension was measured at 600 nm using a microplate reader. Each suspension was measured three times, and each test was conducted three times independently.

*Fourier Transform Infrared Spectroscopy (FTIR)*: The surface chemistry of the ECM, NC, EMH, and EMH-I was characterized using FTIR. FTIR spectra were acquired using an attenuated total internal reflectance Fourier transform infrared (ATR-FTIR) spectroscopy

(Bruker TENSOR II with Platinum ATR Accessory). Each material was measured at least three times by randomly sampling from the bulk to ensure the consistency of the composition.

*Scanning Electron Microscopy (SEM):* A scanning electron microscopy (JCM-6000Plus) was used to visualize the microstructures of tissue samples before and after decellularization, ECM, and ECM-NC gels. For sample preparation, paraffin-embedded sections of native heart and decellularized heart (4 μm) were deparaffinized and air-dried. ECM solution was first gelled at 37 °C and then fixed with 4 % glutaraldehyde, followed by dehydration through a series of ethanol washes (started from 30 % ethanol and ended with 100 % ethanol) and critical point drying (Leica EM CPD300). NC, EMH, and EMH-I were first frozen at -80 °C, followed by lyophilization (Labconco, 0.120 mBar, and -50 °C). All prepared specimens were then sputter-coated with 7 nm gold/palladium (Leica EM ACE200) and imaged using SEM.

*In Vitro Occlusion Model*: The ability of NC, EMH, and EMH-I to withstand physiologically relevant pressure was examined using an in vitro occlusion model according to the previously developed protocol.[8] Briefly, PBS was pumped at 50 mL $min^{-1}$ using a syringe pump to displace the material inside of a tube. The maximum pressure that required displacing 1 mL of the material was recorded as the displacement pressure using a pressure sensor (Omega Engineering Inc., Norwalk, CT). Each test was conducted three times.

*In Vitro Retrieval Test*: The retrievability of EMH-I was tested using a Penumbra System for aspiration (Penumbra, Alameda, CA). The retrieval process was monitored under fluoroscopy (OEC9800 plus C-Arm, GE Healthcare Systems, Chicago, IL).

*Rat Subcutaneous Injections:* All procedures were conducted under animal protocols approved by Mayo Clinic Institutional Animal Care and Use Committee. All animals used in this study

were 4-5 week old Sprague Dawley rats (Charles River Laboratories, Wilmington, MA). 200 µL of saline (control), NC (4.5 wt %), EMH, and EMH-I were subcutaneously injected into lateral pockets of each rat, respectively, under general anesthesia. The rats were sacrificed at day 3, day 14, and day 28 post-implantation, followed by tissue collection for histological examination.

*Arterial and Renal Embolization in a Porcine Model*: All procedures were conducted under animal protocols approved by Mayo Clinic Institutional Animal Care and Use Committee. The procedure was performed according to the previously published protocol.[8] Healthy Yorkshire pigs (S&S Farms, Brentwood, CA) weighing 48 to 55 kg were acclimatized for at least 4 days under standard feeding conditions and suitable temperature. Before the embolization procedure, the pigs were first anesthetized using intramuscular injection of 5 mg $kg^{-1}$ tiletamine-zolazepam (Telazol, Zoetis), 2mg $mL^{-1}$ xylazine, and 0.02 mg $kg^{-1}$ glycopyrrolate. Following intubation, anesthesia was maintained with inhalation of 1.5-3 % isoflurane. During the procedure, percutaneous access to the carotid artery was obtained under the guidance of ultrasound (ACUSON S2000, Siemens) and fluoroscopy (OEC9800 plus C-Arm, GE Healthcare Systems, Chicago, IL). With a 5-French Bernstein catheter (Cook Medical) and a guidewire (GT-glidewire, Terumo Medical), angiography of the internal iliac (n=8) or renal artery (n=8) was performed under real-time fluoroscopic guidance using an intravenous contrast agent (350 mgI $mL^{-1}$ Omnipaque, GE HealthCare, MA). EMH-I was delivered to the iliac or renal artery using a catheter. The radiopacity of EMH-I and vessel patency were assessed using fluoroscopy and digital subtraction angiography, respectively. Repeated angiography was performed to examine the embolic efficacy of EMH-I in vivo. Pigs were either sacrificed 1-hour post-embolization (non-survival group; n=4) or at 2 weeks post-embolization (survival group; n=4). In the survival group, hemostasis at the carotid arterial puncture site was achieved by manual compression and

the wound was sealed using Dermabond (Ethicon, USA). Prior to euthanasia, blood samples were obtained for analysis, and whole-body CT was performed. At necropsy, the embolized internal iliac artery, or the kidneys were removed and examined by microCT and histopathology.

*Complete Blood Count (CBC) and Blood Biochemistry:* CBC was carried out using an automatic analyzer (HemaTrue, Heska, Loveland, CO). CBC was measured to assess the hematological indices in rats and pigs, respectively, to monitor the overall animal health. In addition, blood biochemistry was also evaluated for pigs using a Veterinary Chemistry Analyzer (DRI-CHEM 4000, Heska, Loveland, CO)

*Whole Body CT Scans and Analysis:* The pigs were scanned for embolized artery, and organs, as well as signs of distal migration of embolic agent (EMH-I) using whole-body CT performed on a clinical dual-source scanner (Siemens Force, Siemens Healthineers, Erlangen, Germany). During the scan, CT angiography (CTA) was performed by administrating contrast agent (Omnipaque, 350 mgI $mL^{-1}$, GE HealthCare, MA) intravascularly to visualized vasculature roadmap. The spiral scan was performed at 150 kVp and 80 kVp energy level, respectively, with a 0.6 mm detector size configuration. The segmentation and the volumes of the pig kidneys acquired from CT scans were analyzed using Visage 7.1 (Visage Imaging Inc., San Diego, California).

*Hematoxylin and Eosin (H&E) Staining:* H&E staining (Thermo Fisher Scientific, Cat. # 7111 and 7221, Waltham, MA) was performed according to a previously established protocol[8] on paraffin-embedded sections of cardiac tissues (before and after decellularization), rat subcutaneous tissues, pig vessels, and pig kidneys.

*Masson's Trichrome Staining:* Masson's trichrome staining (Thermo Fisher Scientific, Cat. # 22-110-648, Waltham, MA) was performed according to a previously established protocol[8] on

paraffin-embedded sections of rat subcutaneous tissues and pig iliac arteries to detect connective and muscle tissues.

*Elastic Stain:* Elastic histochemical stain staining (Sigma Aldrich, Cat. # HT25A, St. Louis, MO) was performed according to manufacturer's instructions to identify the internal elastic lamina in explanted pig vessels.

*Immunohistochemistry (IHC):* Immunohistochemical staining for collagen-I, fibronectin, and laminin was performed in cardiac tissue, and EMH-I embolized internal iliac artery at D0 to visualize the presence of extracellular matrix components. For rat subcutaneous injections, myeloperoxidase (MPO) and CD31 were stained. For pig vessels, MPO, and proliferating cell nuclear antigen (PCNA) immunohistochemistry staining were performed following a previously established IHC protocol.[8] briefly, paraffin-embedded sections underwent deparaffinization, endogenous peroxidase quenching, antigen retrieval, and then incubated with 5 % (v/v) goat serum blocking solution (in 1X PBS) for 1 hour at room temperature. For fluorescence IHC, the sections were stained with following antibodies at 4 °C overnight: rabbit polyclonal to Collagen I (Abcam, ab34710, 1:500), mouse monoclonal [IST-9] to Fibronectin (Abcam, ab6328, 1:100), and rabbit polyclonal to Laminin (Abcam, ab11575, 1:200). Alexa Fluor 594 goat anti-mouse IgG (Invitrogen, Cat. # R37121) and Alexa Fluor 594 goat anti-rabbit IgG (Invitrogen, Cat. # A-11037) were used as secondary antibodies. Coverslips were mounted with Antifade Mounting Medium with DAPI (Vectashield, Cat. # H-1200) and imaged using an EVOS FL Auto 2 Imaging System (Thermo Scientific Invitrogen). For colorimetric IHC, the sections were stained with following antibodies at 4 °C overnight: Anti-Myeloperoxidase antibody (Abcam, ab208670, 1:200), Recombinant Anti-CD31 antibody (Abcam, ab182981, 1:200), Recombinant Anti-PCNA antibody (Abcam, ab92552, 1:200). Goat Anti-Rabbit IgG H&L (HRP) (Abcam, ab97051,

1:200) was used as the secondary antibody for 1-hour incubation as room temperature. 3'-Diaminobenzidine [28] substrate (Vector Laboratories, SK-4100) was used for color development, which was monitored under a light microscope. Tissue sections were then counterstained with hematoxylin, dehydrated, mounted, and imaged. Slides with no primary antibodies were included as controls for all samples to confirm the specificity of primary antibodies.

*MicroCT Imaging and Analysis:* Excised pig iliac arteries and kidneys were scanned with a microCT (Skyscan 1276, Bruker Corporation, Kontich, Belgium). The pig iliac arteries were scanned using a current of 200 µA and a voltage of 45 kV with a 0.25 mm aluminum filter at 20 µm resolution and 0.4° rotational step. Harvested pig kidney samples were scanned using a current of 200 µA and a voltage of 55 kV with a 0.5 mm aluminum filter at 80 µm resolution and 0.8° rotational step. The microCT images were then reconstructed using NRcon reconstruction software (Bruker Corporation, Kontich, Belgium) for further analysis.

To acquire the volumes of the embolized EMH-I within the iliac artery, the reconstructed microCT images were loaded into the segmentation software Mimics (Materialise, Leuven Belgium). The EMH-I and connective tissue were segmented based on densities by thresholding. The 3D model of EMH-I was reconstructed, and the volume was generated using 3-Matics (Materialise, Leuven Belgium).

*Statistical Analysis*: Statistical analysis was performed with PRISM 8 (GraphPad Software, San Diego, CA). One-way analysis of variance (ANOVA) with a multiple comparison method was performed for experiments containing more than two groups. Two-way ANOVA analysis followed by Tukey's multiple comparison test was performed For comparison between multiple

groups at multiple time points. The two-tailed, unpaired t-test was performed for experiments with two groups. $p < 0.05$ was defined as statistically significant.

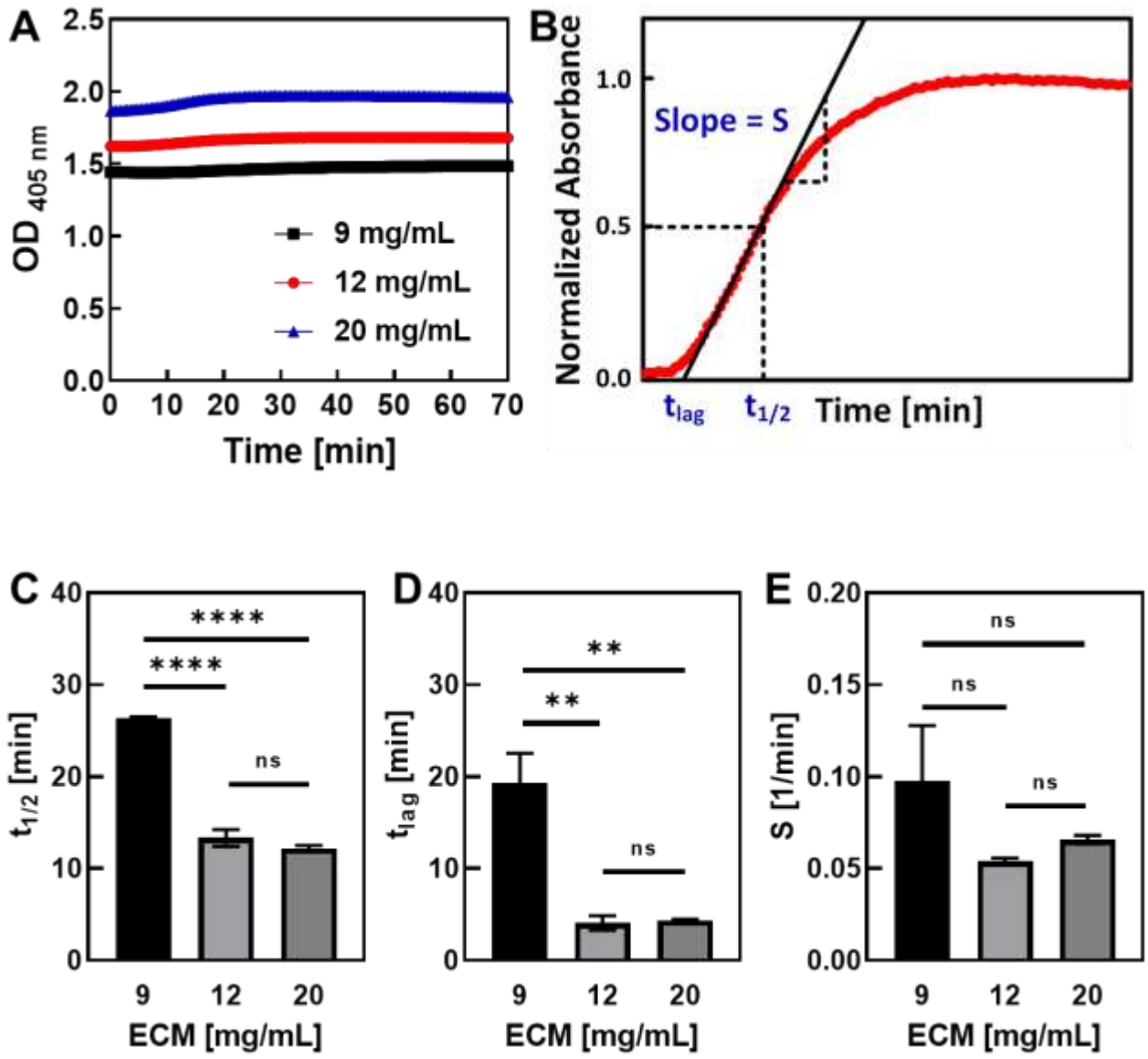


**Figure S1.** (A) Optical density of ECM solutions measured at 405 nm during isothermal gelation at 37 °C. (B) Fitting of the turbidimetric gelation curve to calculate $t_{1/2}$, $t_{lag}$ and $S$. Summary of (C) $t_{1/2}$ , (D) $t_{lag}$ and (E) $S$, of gelation kinetics for ECM of 9, 12 and 20 mg $mL^{-1}$ (n=3). ns, not significant; *$p$ < 0.05, **$p$ < 0.01, ****$p$ < 0.0001. Each data point represents average ± standard error.

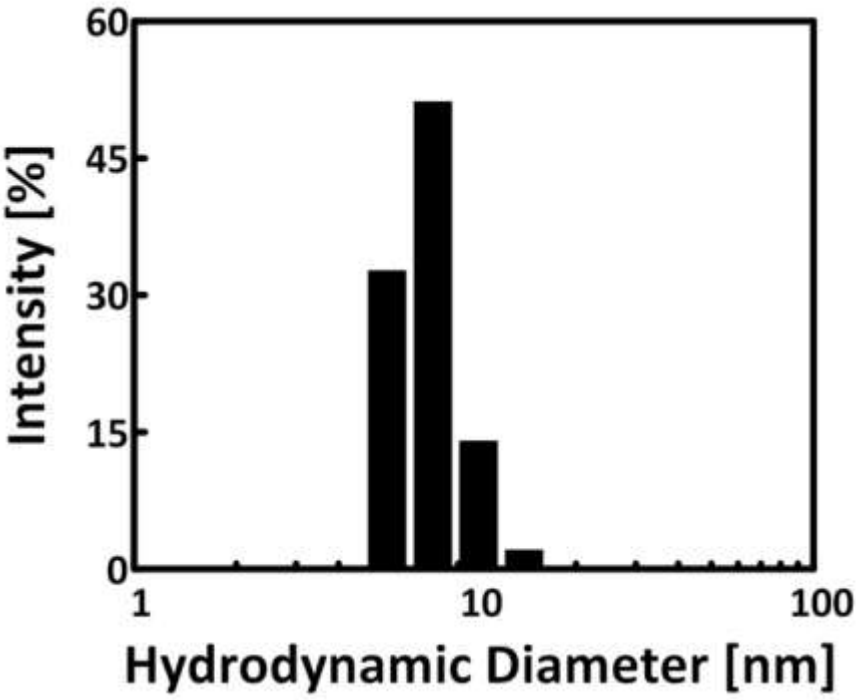


**Figure S2.** Hydrodynamic diameter of NC particles in water measured by dynamic light scattering.

**Table S1.** Summary of xECM4.5NC comprised of 4.5 wt % NC, and varying ECM amount from 0 wt % (3 mg $mL^{-1}$) to 1 wt % (12 mg $mL^{-1}$).

| Gel | ECM [wt%] | ECM [mg $mL^{-1}$] | NC [wt%] | ECM+NC [wt%] | Water [wt%] |
|---|---|---|---|---|---|
| 0ECM4.5NC | 0 | 0 | 4.5 | 4.5 | 95.5 |
| 0.25ECM4.5NC | 0.25 | 3 | 4.5 | 4.75 | 95.25 |
| 0.5ECM4.5NC | 0.5 | 6 | 4.5 | 5 | 95 |
| 0.75ECM4.5NC | 0.75 | 9 | 4.5 | 5.25 | 94.75 |
| 1ECM4.5NC | 1 | 12 | 4.5 | 5.5 | 94.5 |

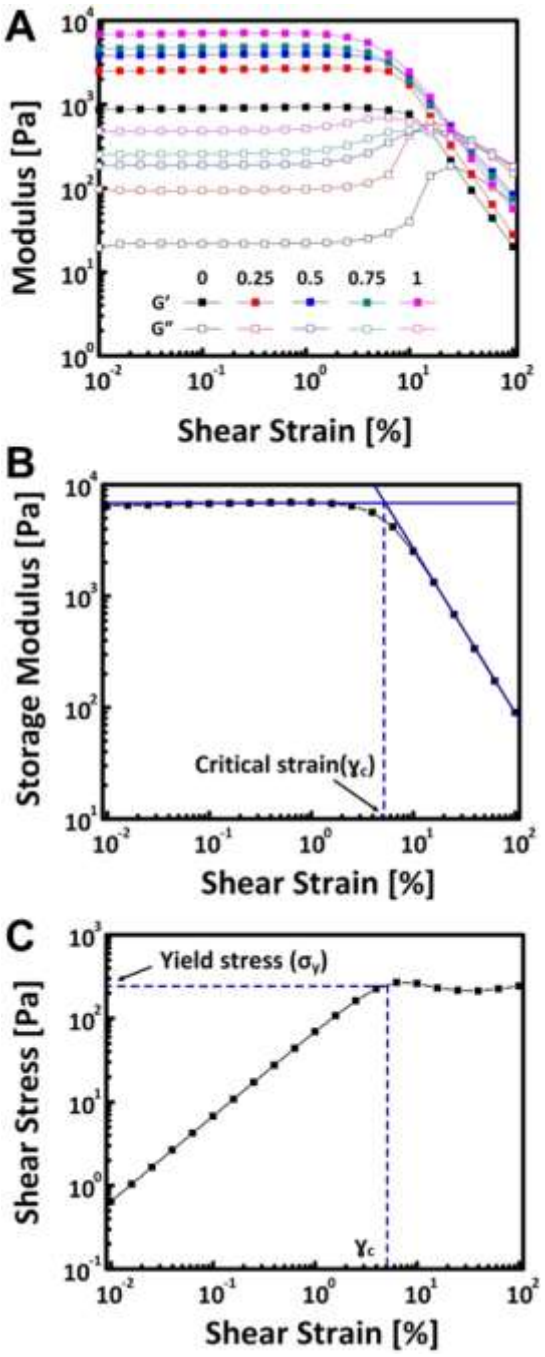


**Figure S3.** (A) Representative amplitude sweeps of the xECM4.5NC gels, showing *G'* and *G"* curves as function of the oscillatory shear strain. Representative schematics showing the calculation procedure of (B) critical strain $\gamma_c$ extracted from *G'* curve, and (C) yield stress $\sigma_y$ extrapolated from stress-strain curve, for each gel.

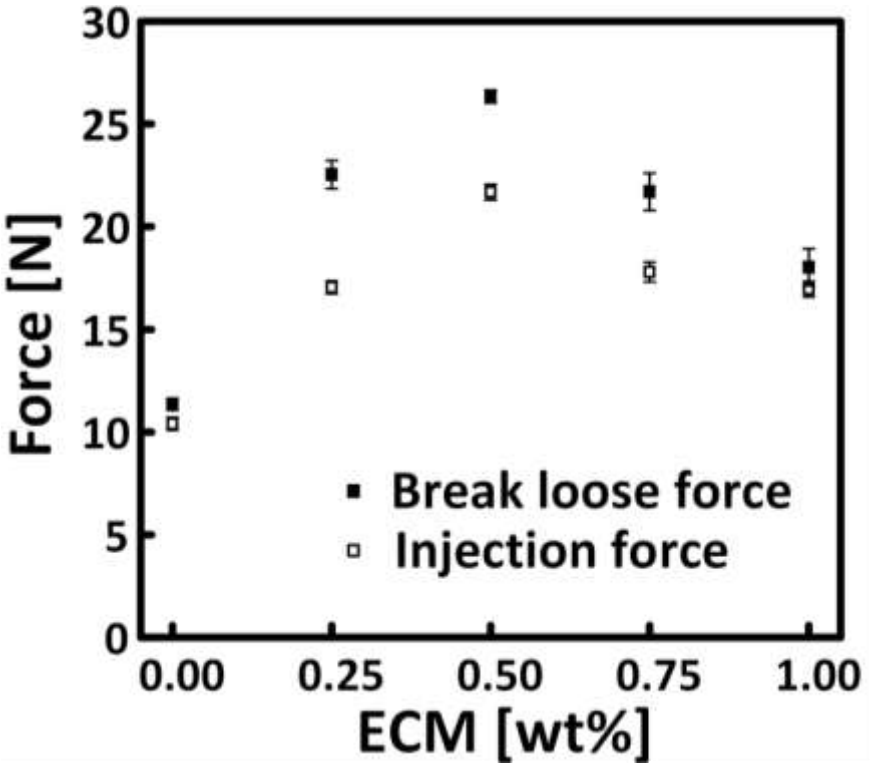


**Figure S4.** Summary of break loose and injection forces of xECM4.5NC nanocomposite gels. The forces suggest the comfortable delivery of the xECM4.5NC gels through 2.8F 110 cm catheter by manual injection.

**Table S2.** Composition summary of ECM-NC nanocomposite hydrogel comprised of a total amount of 5.5 wt% solid, with varying amount of ECM and NC.

| Gel | ECM [wt%] | NC [wt%] | ECM+NC [wt%] | Water [wt%] |
|---|---|---|---|---|
| 0ECM5.5NC | 0 | 5.5 | 5.5 | 94.5 |
| 0.25ECM5.25NC | 0.25 | 5.25 | 5.5 | 94.5 |
| 0.5ECM5NC | 0.5 | 5 | 5.5 | 94.5 |
| 0.75ECM4.75NC | 0.75 | 4.75 | 5.5 | 94.5 |
| 1ECM4.5NC | 1 | 4.5 | 5.5 | 94.5 |

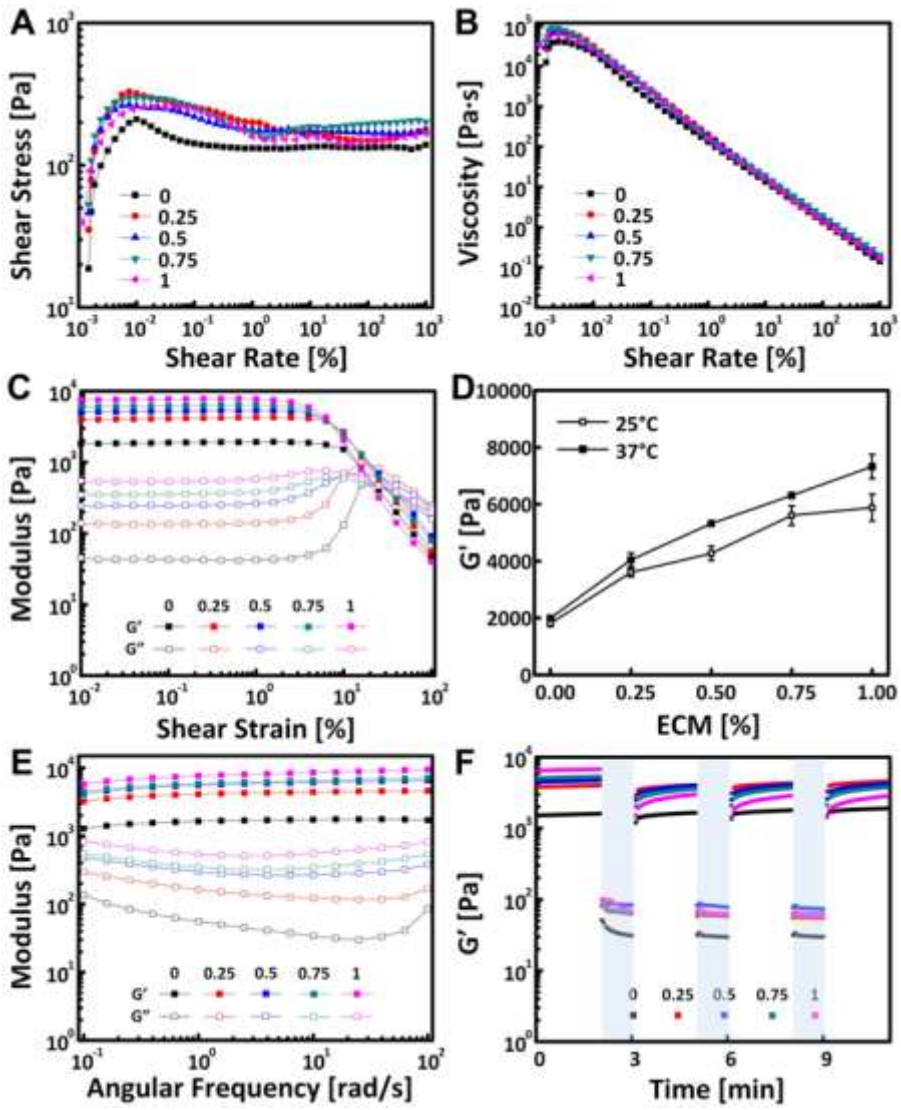


**Figure S5.** Rheology of ECM-NC gels with 5.5 wt % of total solid content. (A) Time-dependent plots of shear stress versus shear rate. (B) Shear-rate sweeps, showing shear-thinning properties. (C) Amplitude sweeps performed at 10 rad $s^{-1}$. (D) Summary of G′ at 25 °C and 37 °C (n=3). *G'* increased with increased ECM amount and decreased NC content. (E) Oscillatory frequency sweeps performed at 10 rad $s^{-1}$ at 0.1 % strain. (F) Thixotropy test, showing recoverability of the gels. Deformation and recovery of gels evolved over time from repeated cycles of 2-minute low 0.1 % strain and 1-minute high 100 % strain oscillations at 10 rad $s^{-1}$.

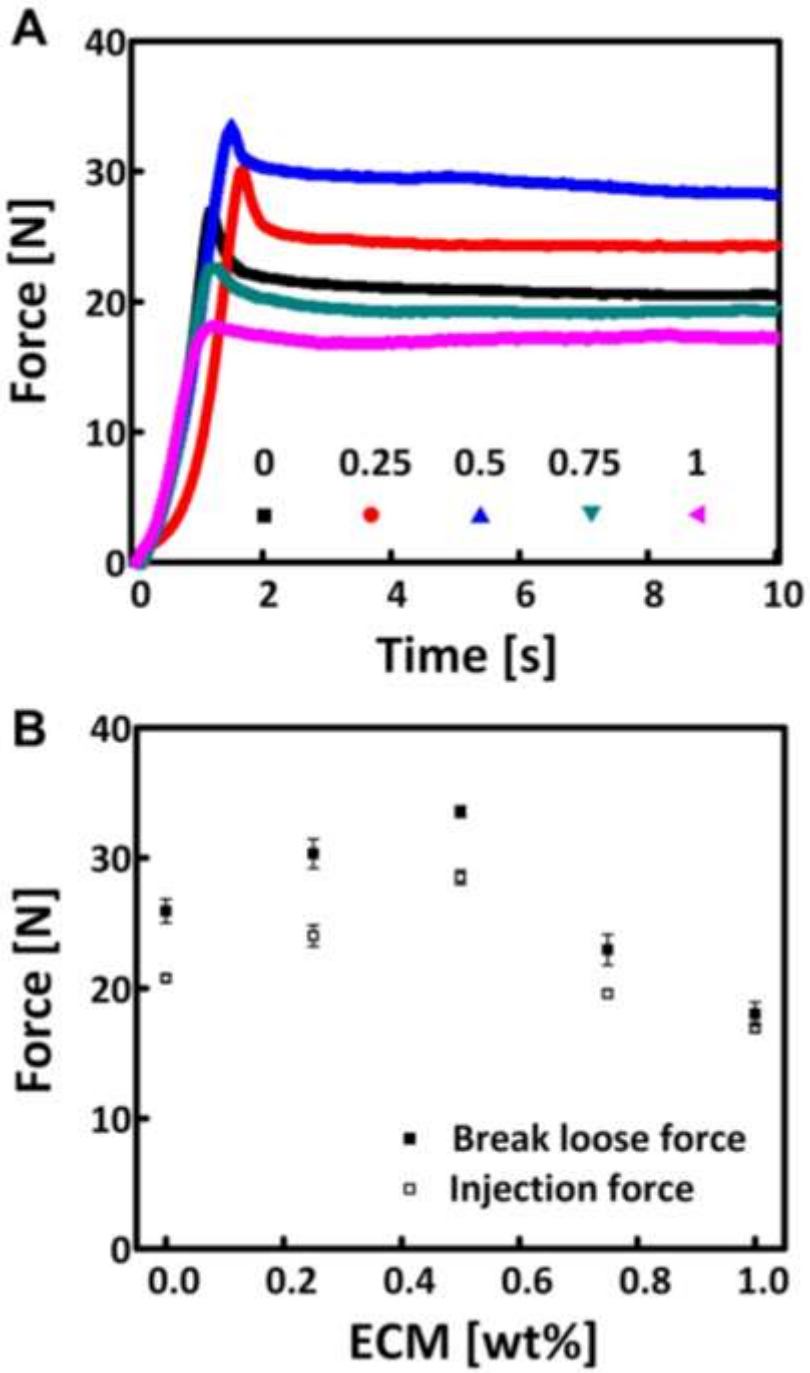


**Figure S6.** (A) Representative injection curve of ECM-NC gels with a constant total solid amount of 5.5 wt %. (B) Summary of break loose force and injection force (n=5). The forces indicate the comfortable delivery of the formulated gels through a 2.8F 110 cm catheter by manual injection.

**Table S3.** Summary of radiopaque xECM4.5NC-I gels comprised of 4.5 wt% NC, 27 wt% iohexol and varying ECM amount from 0 wt% (0 mg $mL^{-1}$) to 1 wt% (12 mg $mL^{-1}$).

| Gel | ECM [wt%] | ECM [mg $mL^{-1}$] | NC [wt%] | ECM+NC [wt%] | Iohexol [wt%] |
|---|---|---|---|---|---|
| 0ECM4.5NC-I | 0 | 0 | 4.5 | 4.5 | 27 |
| 0.25ECM4.5NC-I | 0.25 | 3 | 4.5 | 4.75 | 27 |
| 0.5ECM4.5NC-I | 0.5 | 6 | 4.5 | 5 | 27 |
| 0.75ECM4.5NC-I | 0.75 | 9 | 4.5 | 5.25 | 27 |
| 1ECM4.5NC-I | 1 | 12 | 4.5 | 5.5 | 27 |

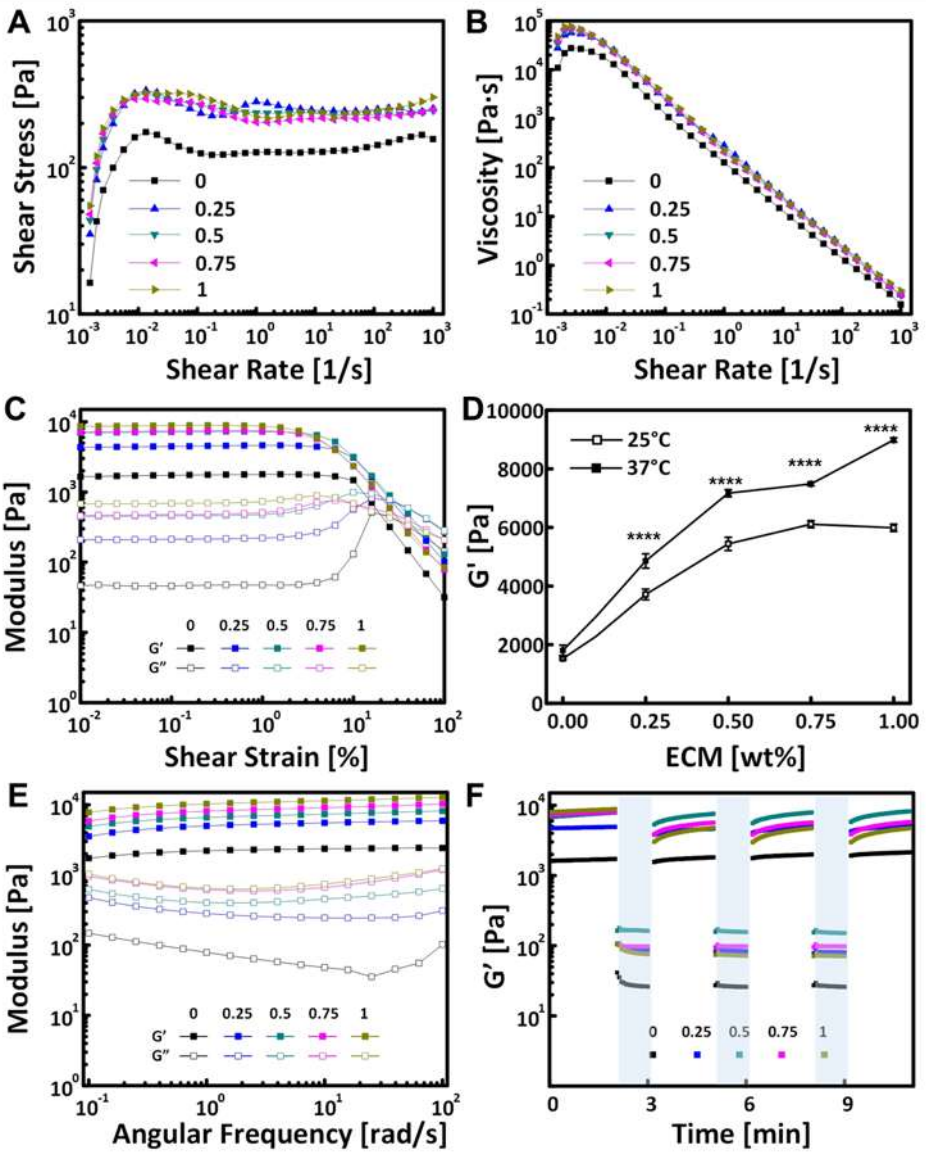


**Figure S7.** Rheological properties of radiopaque xECM4.5NC-I gels. (A) Time-dependent plots of shear stress versus shear rate. (B) Shear-rate sweeps, showing shear-thinning properties. (C) Amplitude sweeps performed at 10 rad $s^{-1}$. (D) Summary of *G'* at 25 °C and 37 °C (n=3). G′ increased with increased ECM amount at constant NC content. (E) Oscillatory frequency sweeps performed at 10 rad $s^{-1}$ at 0.1% strain. (F) Thixotropy test, showing recoverability of radiopaque xECM4.5NC-I gels. Deformation and recovery of gels evolved over time from repeated cycles of 2-minute low 0.1 % strain and 1-minute high 100 % strain oscillations at 10 rad $s^{-1}$.

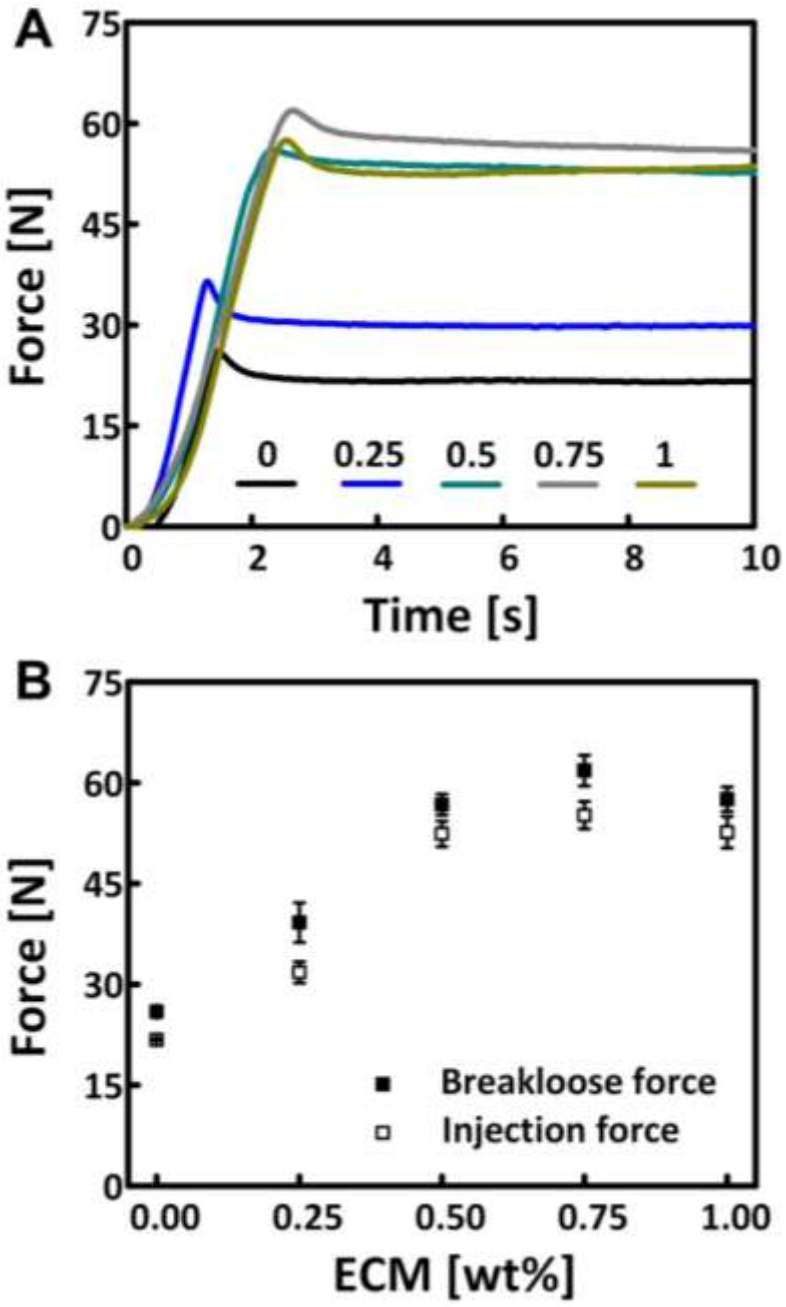


**Figure S8.** (A) Representative injection curves of radiopaque xECM4.5NC-I gels. (B) Summary of break loose force and injection forces (n=5). The forces reveal the comfortable delivery of the xECM4.5NC-I gels through 2.8F 110 cm catheter by manual injection.

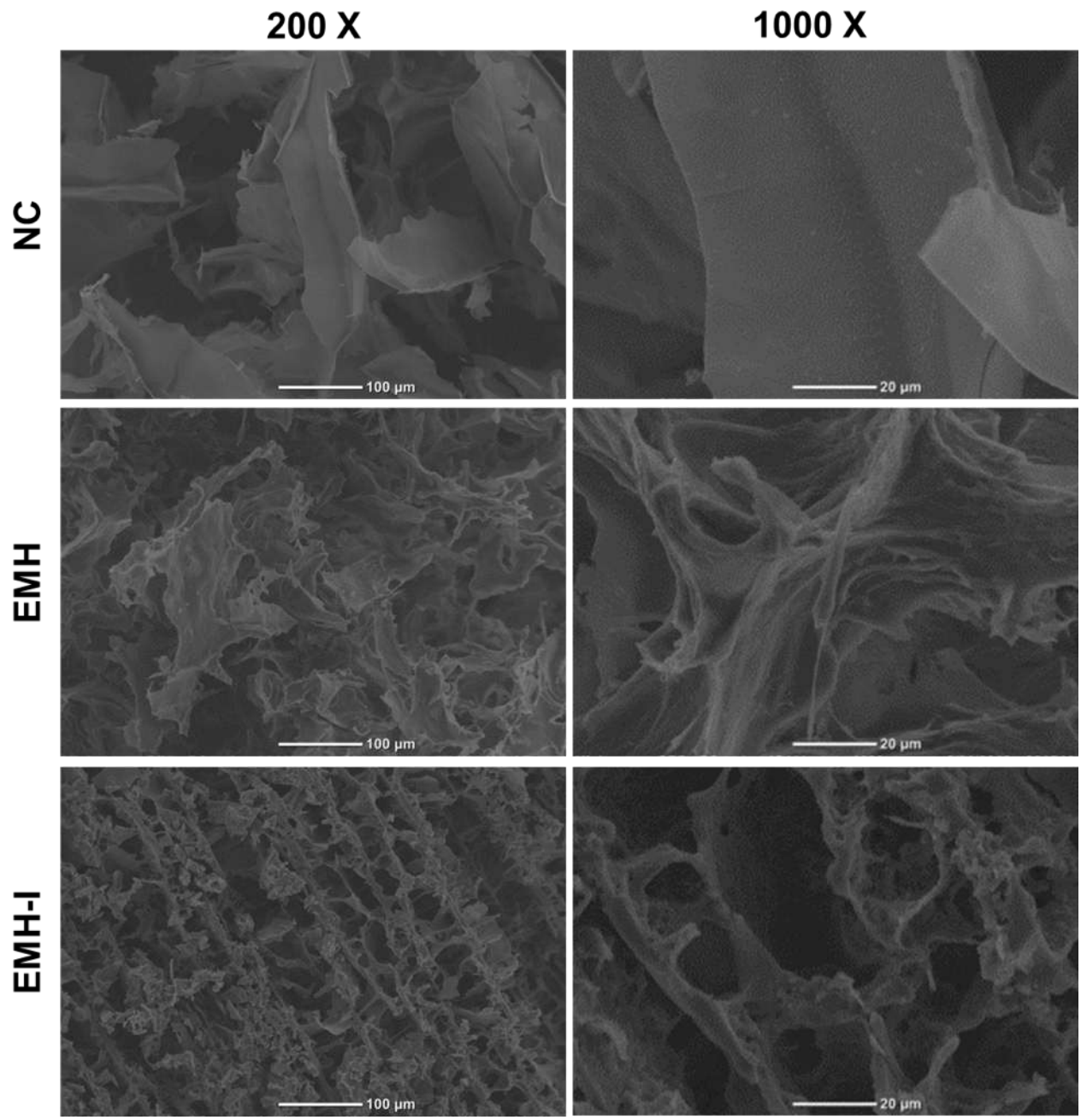


**Figure S9.** Representative SEM images of NC, EMH, and EMH-I at high and low magnifications. NC had a relatively large flaky, and non-connective structure. When ECM was added into NC, the formed EMH appeared to be compact with struts that connected the adjacent structures. With the addition of iohexol into EMH, formulated EMH-I showed a porous, dense, and organized structure, which gave rise to its enhanced mechanical property.

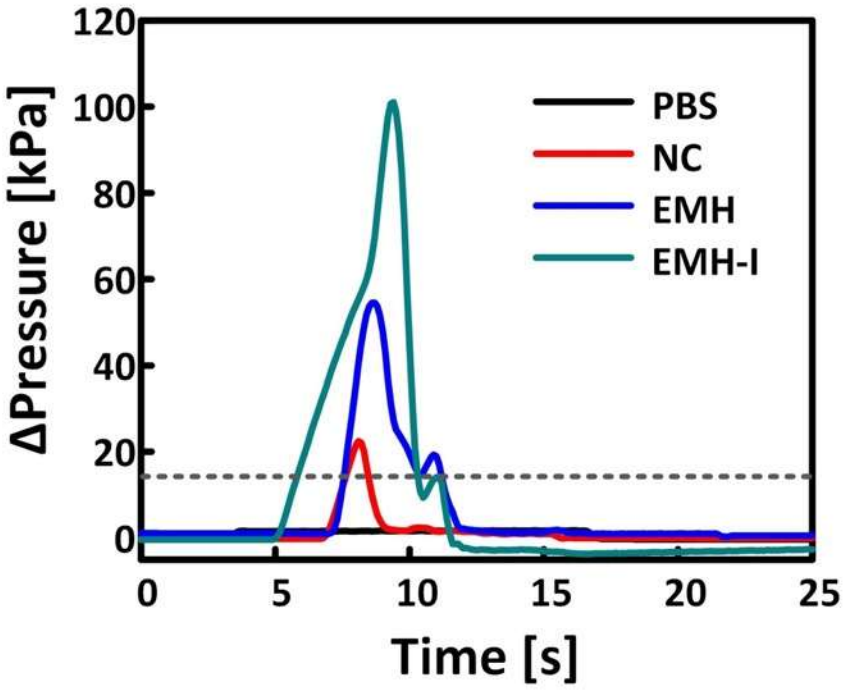


**Figure S10.** Representative pressure displacement curves of PBS (control), NC, EMH, and EMH-I. The peak force corresponded to the maximum pressure each material can withstand at a flow rate of 50 mL $min^{-1}$. EMH-I showed the highest pressure, followed by EMH and NC. At least 4-fold and 7-fold of physiological pressure is required to displace EMH and EMH-I, respectively. The dotted line represented the physiological pressure of 16 kPa, equivalent to 120 mmHg.

**Table S4.** Summary of complete blood count (CBC) for subcutaneously injected rats. Rats were healthy, and no infection was observed. Each data point represents average ± standard error (n=4). The statistics is presented in Figure S11.

| Parameter | Day 0 | Day 3 | Day 14 | Day 28 |
|---|---|---|---|---|
| White Blood Cell (WBC) [$10^3$ $\mu L^{-1}$] | 12.1 ± 0.8 | 9.1 ± 0.3 | 10.6 ± 0.1 | 9.9 ± 0.3 |
| Lymphocyte (LYM) [$10^3$ $\mu L^{-1}$] | 9.4 ± 0.5 | 6.0 ± 0.3 | 7.8 ± 0.1 | 7.5 ± 0.3 |
| Monocyte (MONO) [$10^3$ $\mu L^{-1}$] | 0.6 ± 0.0 | 0.6 ± 0.0 | 0.5 ± 0.0 | 0.4 ± 0.0 |
| Granulocyte (GRAN) [$10^3$ $\mu L^{-1}$] | 2.1 ± 0.2 | 3.3 ± 0.1 | 2.3 ± 0.0 | 2.0 ± 0.1 |
| Red Blood Cell (RBC) [$10^6$ $\mu L^{-1}$] | 6.9 ± 0.1 | 6.9 ± 0.1 | 7.4 ± 0.0 | 7.1 ± 0.1 |
| Platelet (PLT) [$10^3$ $\mu L^{-1}$] | 284.3 ± 26.1 | 340.8 ± 19.0 | 246.2 ± 10.2 | 224.5 ± 11.9 |

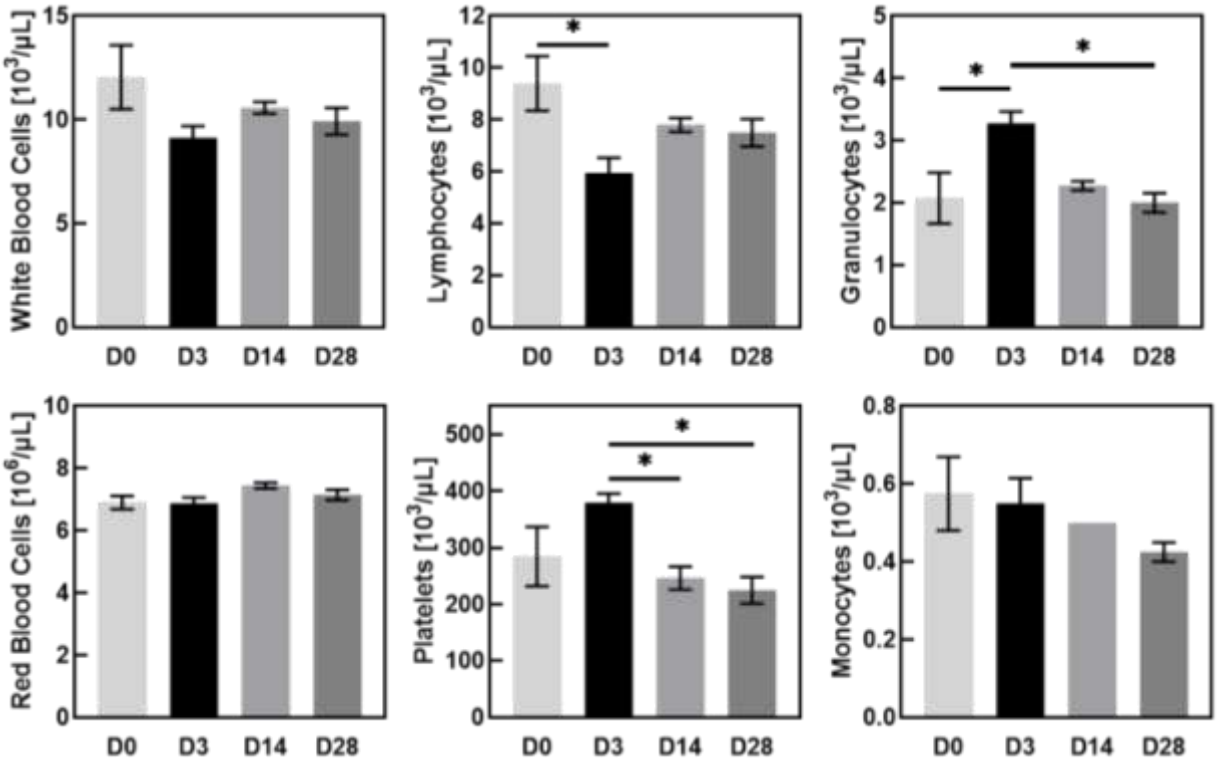


**Figure S11.** Graphic summary of CBC parameters of subcutaneously injected rats at D0, D3, D14, and D28. *$p < 0.05$. Rats were healthy, and no infection was observed. Each data point represents the average ± standard error (n=4).

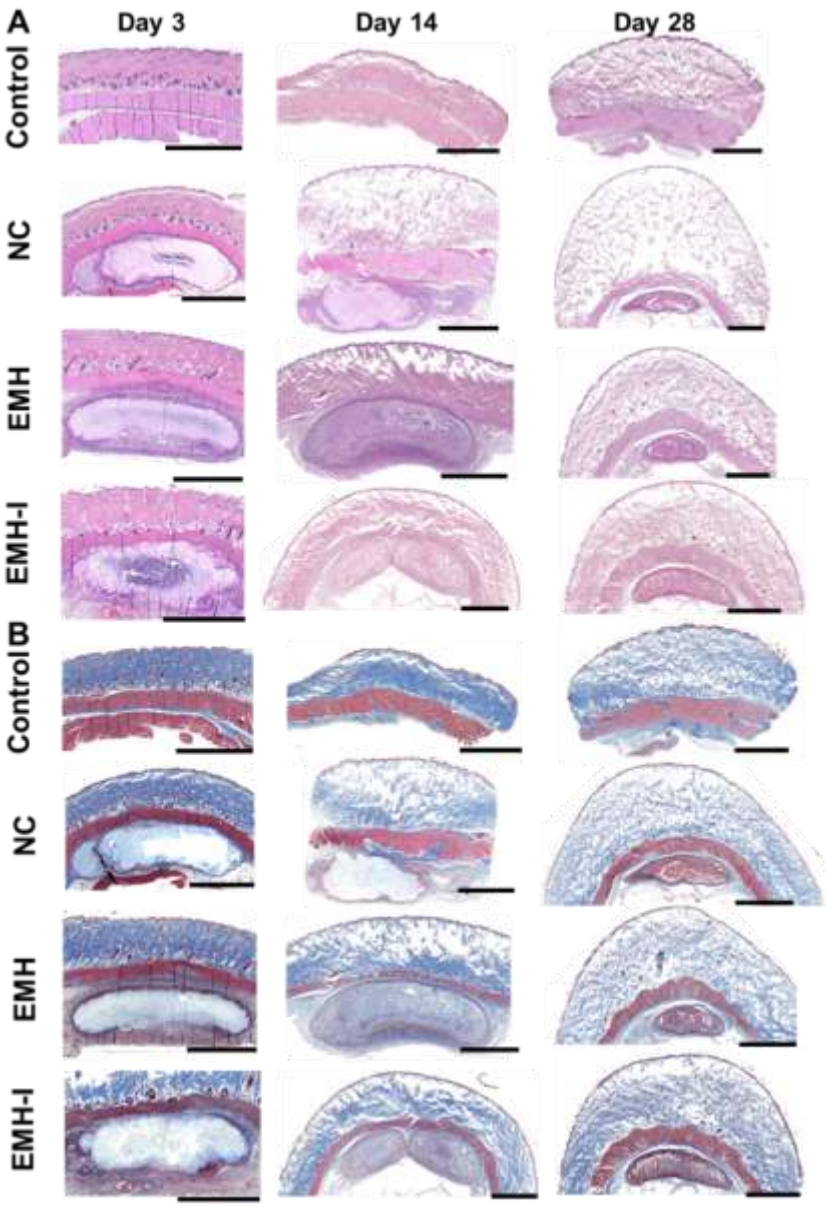


**Figure S12.** Representative histological images of subcutaneously injected NC, EMH, EMH-I, and control (saline injection) in rats 3, 14, and 28 days post-injection (A) H&E staining; and (B) Masson's Trichrome staining. A downward trend was observed in the cross-sectional area of explanted NC, EMH, and EMH-I over 28 days. Note that the fracturing of the dermis, with increased clear space, is due to processing artifact, as reviewed by a board-certified pathologist. Bar scales for all images are 3 mm.

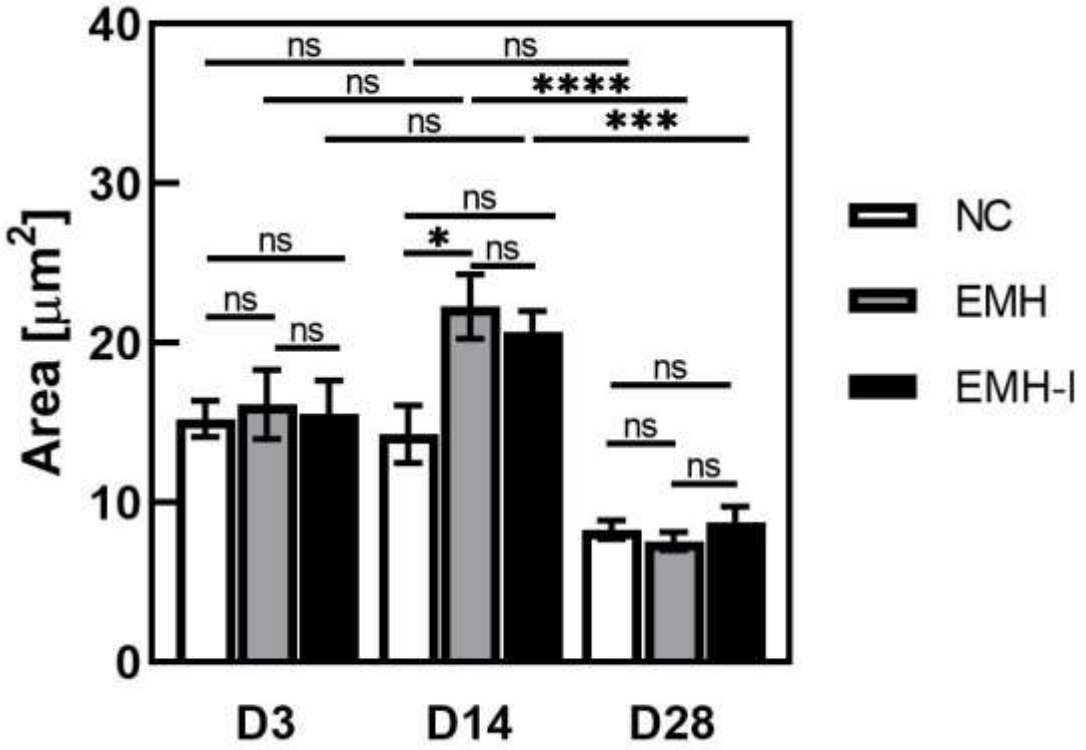


**Figure S13.** The cross-sectional area of explanted NC, EMH, and EMH-I at 3, 14, and 28 days post subcutaneous injection (n=4). *$p$ < 0.05. All materials underwent gradual in vivo degradation. Each data point represents the average ± standard error.

**Table S5.** Complete blood count and biochemistry for pigs underwent embolization at D0 and D14. Pigs were healthy, and no infection was observed. ns, not significant; *$p < 0.05$, **$p < 0.01$, ***$p < 0.005$. Each data point represents the average ± standard error (n=4).

| Parameter | Day 0 | Day 14 | p value | Significance |
|---|---|---|---|---|
| Total Protein (TP) [g $dL^{-1}$] | 5.4 ± 0.2 | 7.0 ± 0.1 | 0.0005 | *** |
| Alkaline Phosphatase (ALP) [U $I^{-1}$] | 138.5 ± 23.7 | 126 ± 13.0 | 0.4165 | ns |
| Glucose (GLU) [mg $dL^{-1}$] | 116.0 ± 5.0 | 87.5 ± 3.7 | 0.0466 | * |
| Alanine Aminotransferase (ALT) [U $L^{-1}$] | 39.0 ± 5.8 | 43.0 ± 1.4 | 0.5697 | ns |
| Creatinine (CRE) [mg $dL^{-1}$] | 1.3 ± 0.2 | 1.6 ± 0.2 | 0.1514 | ns |
| Blood Urea Nitrogen (BUN) [mg $dL^{-1}$] | 12.5 ± 2.1 | 11.4 ± 1.1 | 0.5737 | ns |
| White Blood Cell (WBC) [$10^3$ $\mu L^{-1}$] | 13.4 ± 2.6 | 16.7 ± 5.8 | 0.4990 | ns |
| Lymphocyte (LYM) [$10^3$ $\mu L^{-1}$] | 7.5 ± 1.5 | 7.2 ± 1.4 | 0.7177 | ns |
| Monocyte (MONO) [$10^3$ $\mu L^{-1}$] | 0.7 ± 0.1 | 1.6 ± 0.8 | 0.3246 | ns |
| Granulocyte (GRAN) [$10^3$ $\mu L^{-1}$] | 5.2 ± 1.3 | 7.9 ± 4.1 | 0.5354 | ns |
| Hematocrit (HCT) [%] | 23.0 ± 1.9 | 22.7 ± 2.3 | 0.9423 | ns |
| Red Blood Cell (RBC) [$10^6$ $\mu L^{-1}$] | 4.9 ± 0.4 | 4.8 ± 0.5 | 0.9131 | ns |
| Platelet (PLT) [$10^3$ $\mu L^{-1}$] | 266.8 ± 36.2 | 292.3 ± 65.4 | 0.4662 | ns |

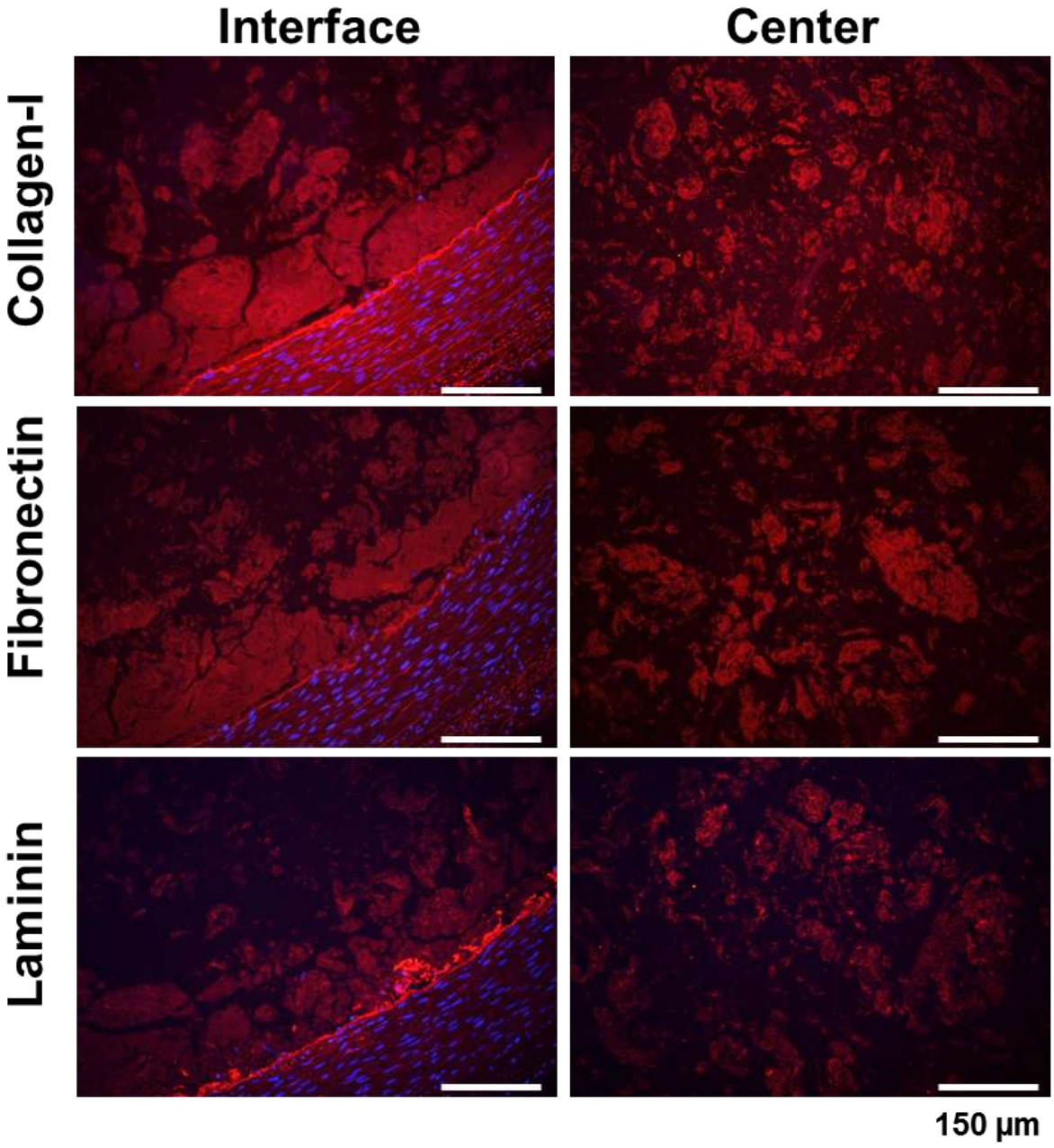


**Figure S14.** Representative immunohistochemistry images of EMH-I in embolized iliac artery focusing at vessel/EMH-I interface and vessel center for collagen-I, fibronectin, and laminin at D0. These images confirmed the preservation of critical ECM proteins in EMH-I gels when used for embolization.

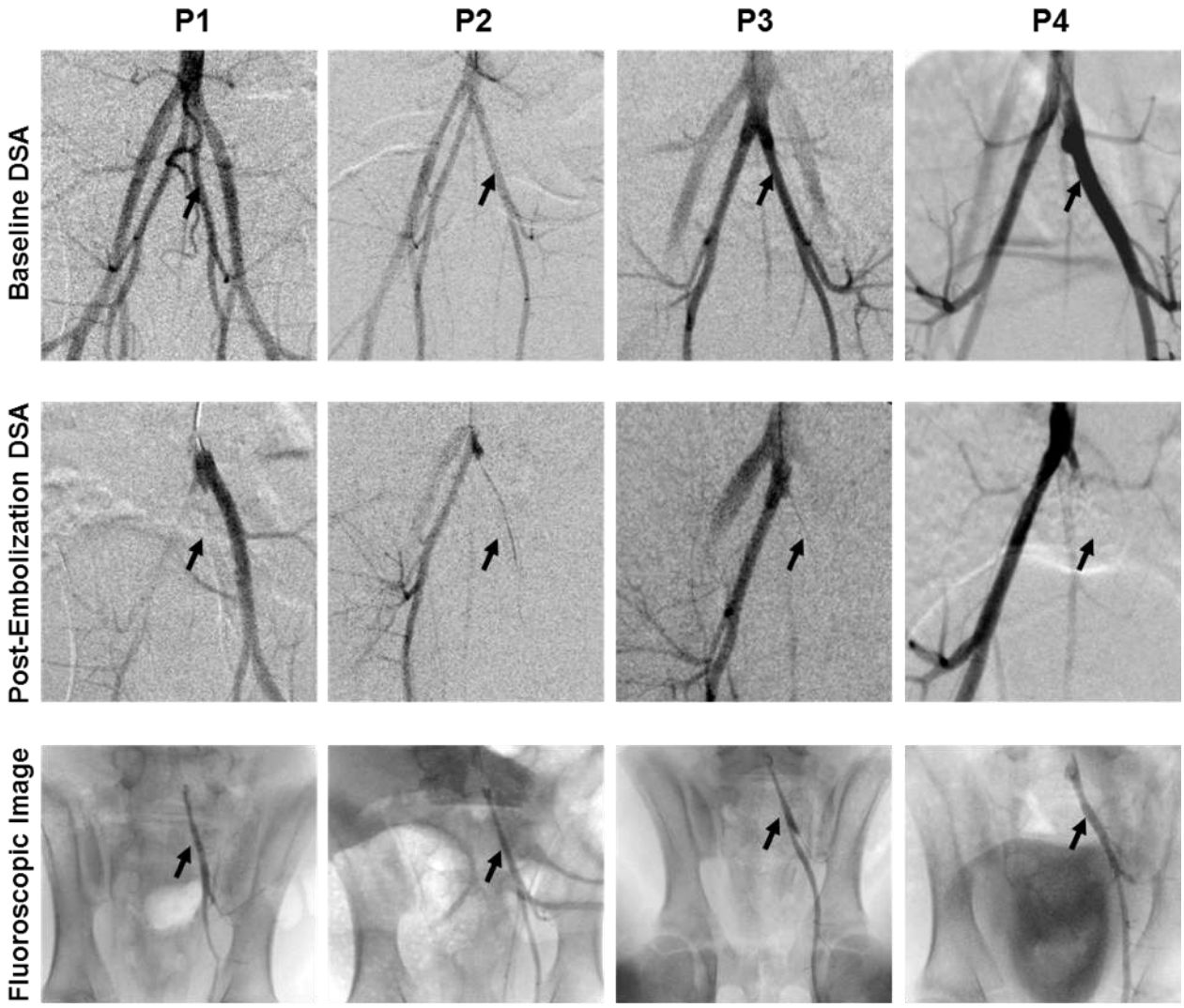


**Figure S15.** Arterial embolization showing baseline DSA, post-embolization DSA, and fluoroscopic image of EMH-I in IIAs of four pigs, P1, P2, P3, and P4, showing complete occlusion and successful embolization in all animals. Fluoroscopic images demonstrate the embolized IIA because the EMH-I contains iohexol. Black arrows represent the IIA. Note that the arrows in P2 and P3, post-embolization DSA panel, point to the completely occluded IIA; linear opacification seen in the images is an accessory arterial branch that is superimposed.

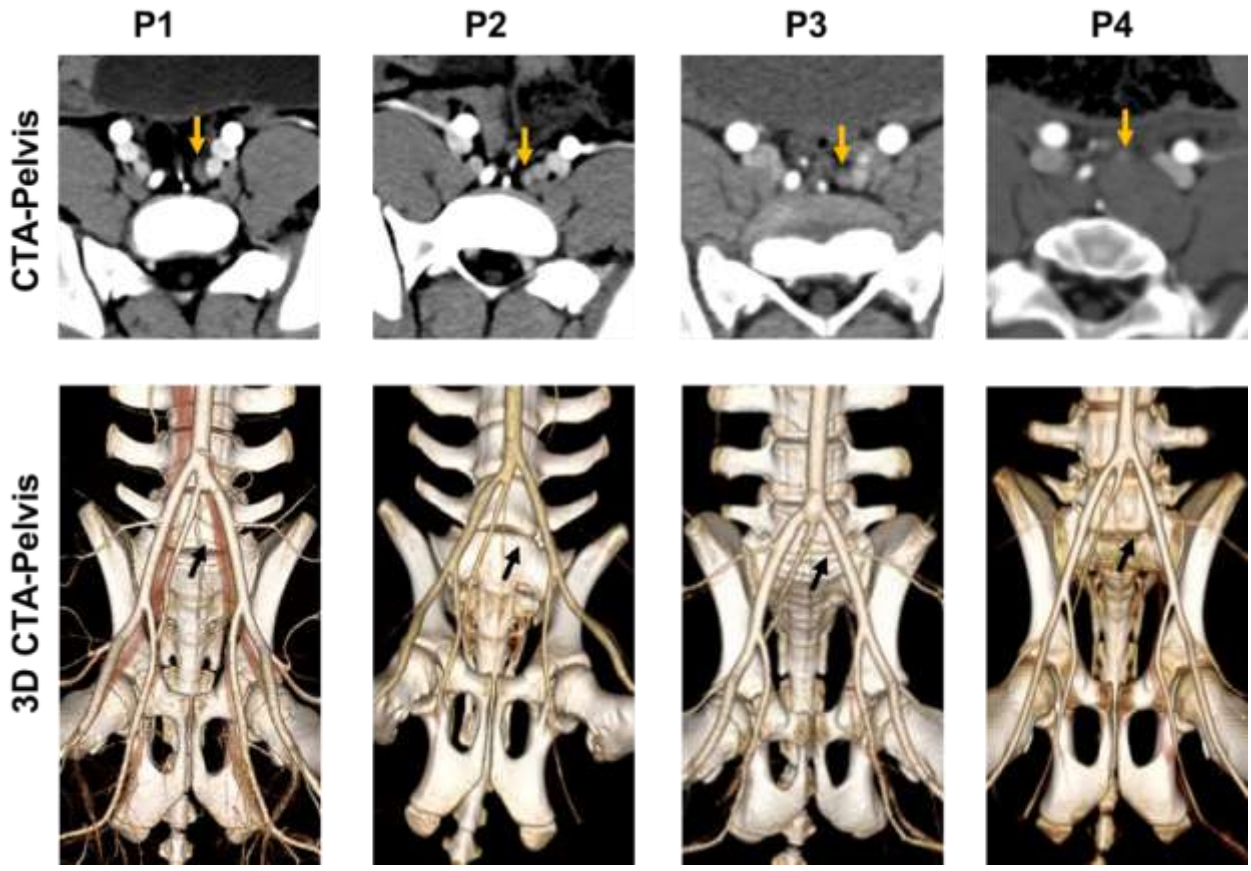


**Figure S16.** CTA and 3D CTA pelvis images acquired 14 days post arterial embolization, showing complete occlusion of IIA for all 4 animals. Orange arrows indicate the embolized artery in CTA, and black arrows indicate the embolized artery not visualized in the 3D CTA due to lack of blood flow from embolization.

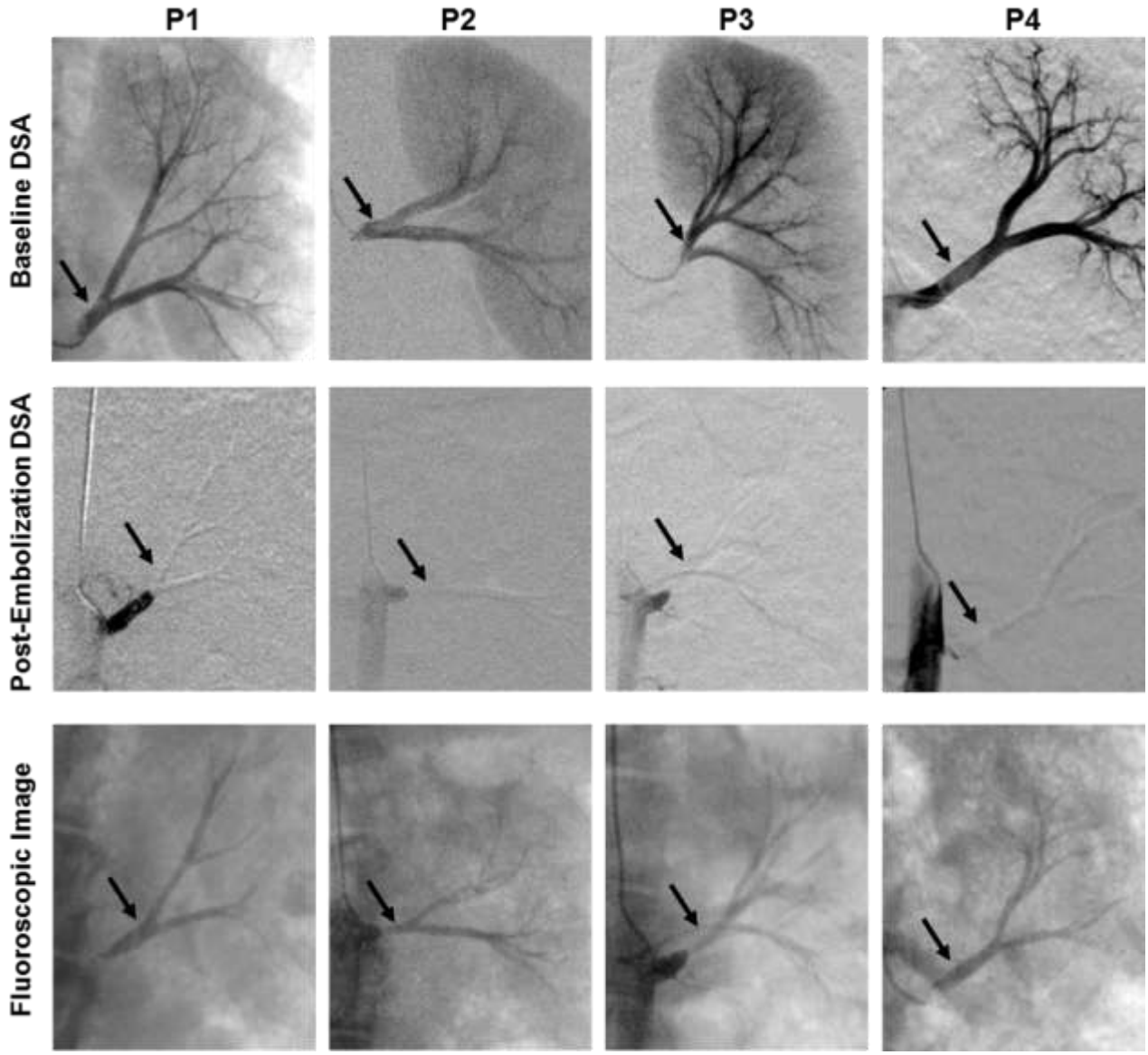


**Figure S17.** Porcine renal artery embolization showing baseline DSA, post-embolization DSA, and fluoroscopic image of EMH-I in renal vasculatures for four pigs, P1, P2, P3, and P4. The missing renal vasculature after EMH-I infusion confirmed successful embolization in all four pigs. Fluoroscopic images demonstrate the EMH-I within the artery; they are visible under x-ray because they contain iohexol. Black arrows indicate the main renal artery.

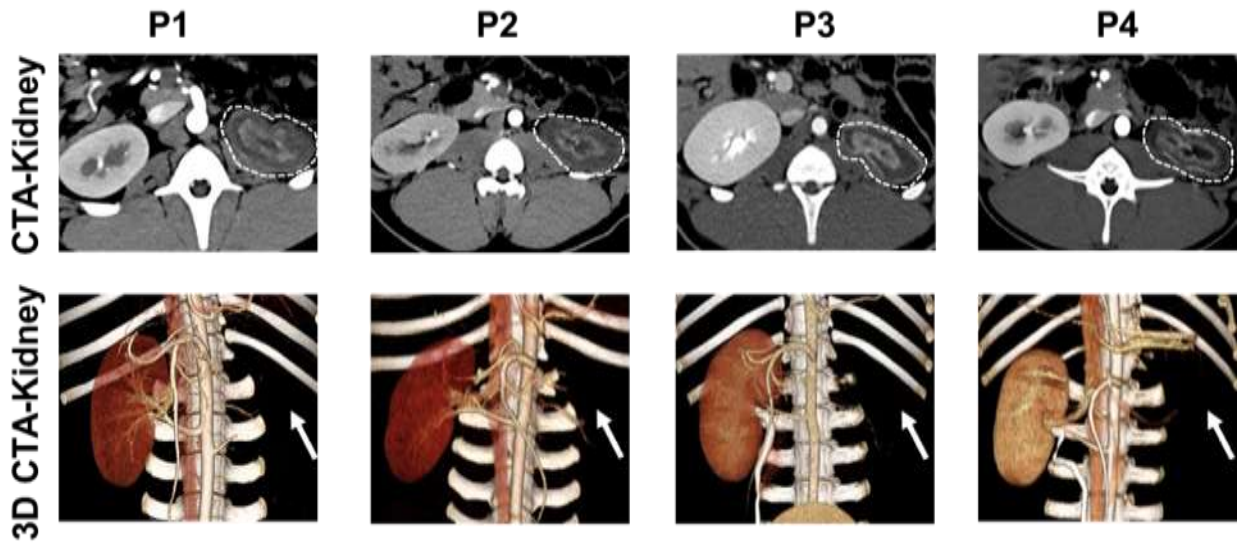


**Figure S18.** CTA images acquired 14 days post renal artery embolization. The embolized kidney (white dotted outline) demonstrates absence of enhancement and appears smaller in size compared to contralateral normal kidney in all four animals. Corresponding 3D CTA images indicate absence of the embolized kidneys (white arrows), confirming successful renal artery embolization.

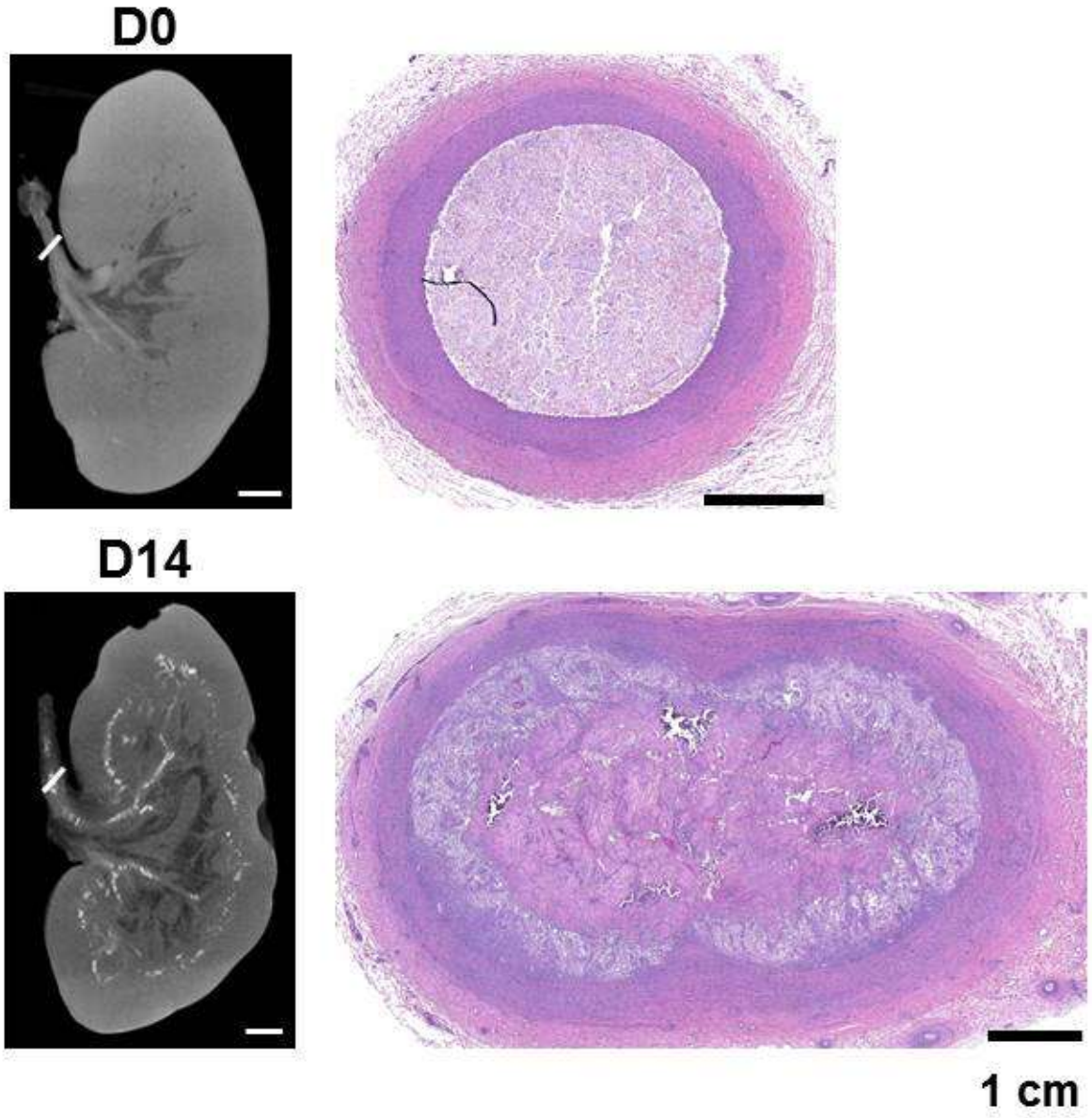


**Figure S19.** Representative microCT images of embolized kidneys collected at day 0 and day 14 after EMH-I embolization. H&E staining of the renal artery (location marked by white line) showed occlusion at D0 and persistent occlusion with evidence for remodeling of the renal artery at D14. D14 sample shows circumferential degradation of the biomaterial and connective tissue deposition with residual EMH-I centrally.

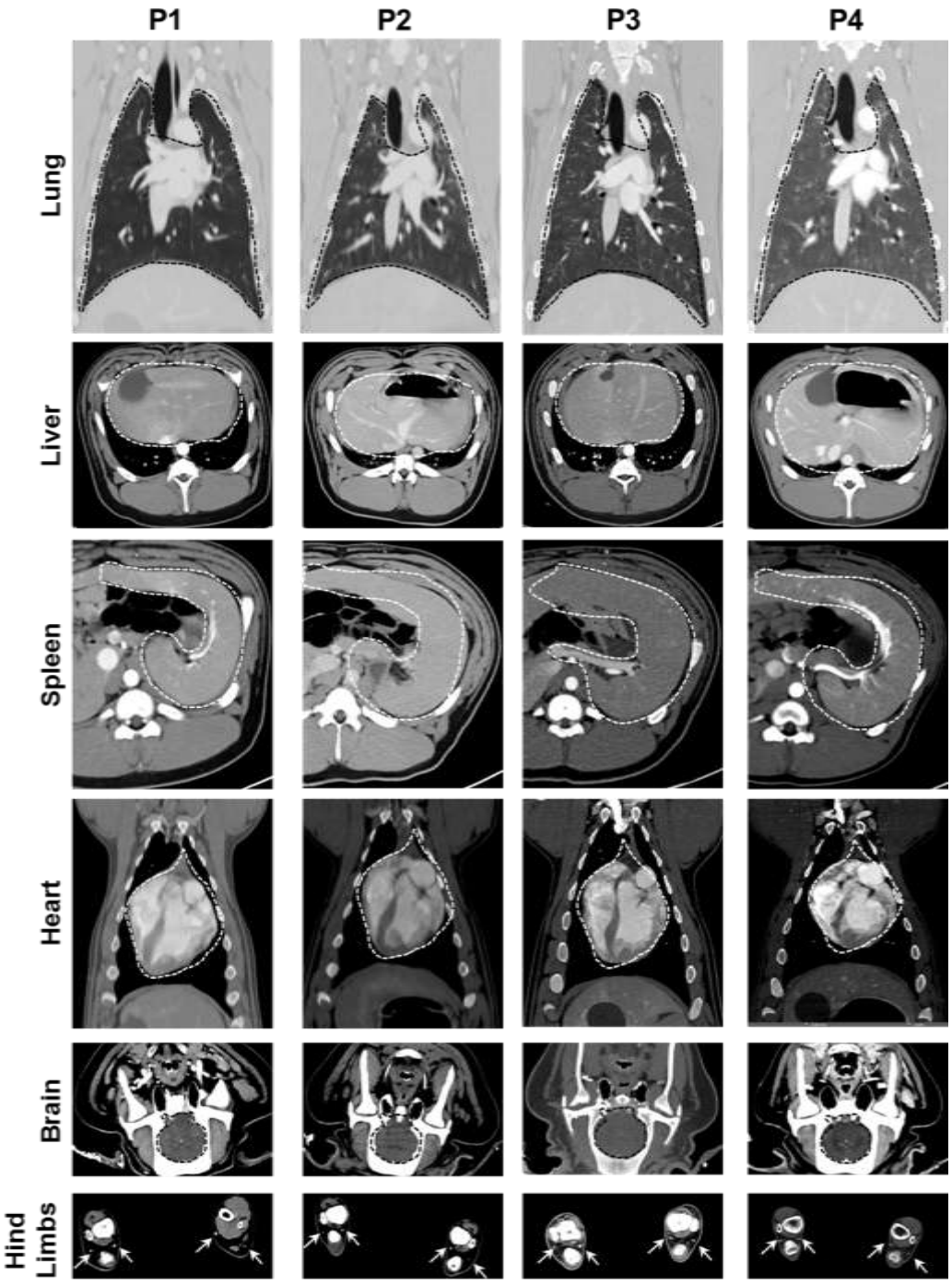


**Figure S20.** CT images acquired 14 days post embolization in the porcine model, showing normal findings with preserved hindlimb perfusion in all four animals. Lung, liver, spleen, heart, and brain are outlined by dotted line. White arrows indicate widely patent distal hindlimb vessels.

**Video S1.** *In vitro* retrieval of EMH-I using an 8 French aspiration catheter in a vessel model in real time. The top section shows that the EMH-I placed in the middle of the vessel model is retrieved gradually by the aspiration catheter. The process is also monitored under X-ray based fluoroscopy (bottom section), where the radiopaque EMH-I is shown to be dark.